

Banner appropriate to article type will appear here in typeset article

Flow Development in the Entrance Region of Slender Converging Pipes

Vinicius M. Sauer[†]

Department of Mechanical Engineering, California State University, Northridge, CA 91330, USA

(Received xx; revised xx; accepted xx)

The hydrodynamic entrance region in internal conduits, where the velocity profile evolves to a fully developed state, is a classical problem in fluid mechanics. Although many fundamental studies involve developing flows in circular ducts with constant area – for which several theoretical descriptions exist – converging pipe sections are often employed, demanding the extension of the analysis to pipes with slowly varying areas. This work presents an analytical investigation of the hydrodynamic entrance region in laminar axisymmetric flows through slender converging pipes at moderate Reynolds numbers. The theoretical model extends the recent analysis for developing flows in straight pipes by adopting a classical approach where the flow is divided radially into two regions: a wall region, where viscous effects are dominant and advection is neglected, and a central core, where both inertia and viscous effects are considered. The effects of the inlet Reynolds number and the inlet angle on the developing velocity profile and pressure drop are analysed. Results show that a converging geometry, which imposes a favourable pressure gradient, shortens the hydrodynamic entrance length compared to a straight pipe at the same inlet Reynolds number. The analytical solutions for the evolution of the velocity field are validated against numerical simulations of the full Navier-Stokes equations, showing good agreement. The model provides a concise theoretical description of the interaction between boundary-layer development and pressure gradients in the entrance region of laminar flows in slender converging pipes.

Key words: –

1. Introduction

The study of internal fluid flow in conduits with varying cross-sections is a classical problem of fundamental importance. Beyond its fundamental role in viscous–inertial interactions, it is of practical relevance in various contexts, including propulsion systems, diffusers and nozzles, heat exchangers, and physiological transport processes. Although the entrance flow in a straight, uniform pipe is a canonical problem, the interaction between the developing boundary layer and the pressure gradients imposed by a varying geometry introduces more complexity. In a converging section, a favourable pressure gradient accelerates the core flow.

[†] Email address for correspondence: vmsauer@csun.edu

A central aspect of such internal flows is the hydrodynamic entrance region, where the velocity profile evolves from its initial state at the inlet to a fully developed, invariant form.

The case of a straight circular pipe has been particularly well studied, forming the basis of classical entrance-region theory. Early work by Langhaar (1942) provided one of the first systematic descriptions of the “transition length” by linearizing the governing equations and deriving approximate relations for pressure loss. This approach was refined by Campbell & Slattery (1963), who emphasized the structure of the entrance profile, and by Lundgren *et al.* (1964), who derived general expressions for the entrance-region pressure drop applicable to ducts of arbitrary cross-section. Further studies addressed specific geometries, including annular ducts (Sparrow & Lin 1964) and rectangular sections (Sparrow *et al.* 1964; McComas 1967), and extended the framework to heat transfer problems (Kakaç & Özgü 1969).

Asymptotic and analytical techniques also contributed significantly to the theoretical description of developing laminar flows. Van Dyke (1970) constructed uniformly valid asymptotic solutions for channel entry flows at high Reynolds number, while Fargie & Martin (1971) and Mohanty & Asthana (1979) further clarified the subdivision of the entrance into an inviscid core and viscous near-wall subregions. More recently, Durst *et al.* (2005) revisited the problem with careful experiments and simulations, refining entrance-length correlations. Most notably, (Kim 2024) introduced a new analytical solution to the parabolised Navier–Stokes equations for developing laminar pipe flow, which demonstrated that the approach to similarity is not monotonic but involves a near-wall velocity overshoot – an effect overlooked in earlier models. This refinement provides a crucial starting point for further theoretical developments.

In contrast, the corresponding theory for ducts with slowly varying cross-sectional area remains less developed, despite their ubiquity. The classical Jeffery–Hamel solution (Jeffery 1915; Hamel 1917) describes laminar flow in a two-dimensional wedge and illustrates the inherent tendency of diverging flows toward separation. Yet, its idealized geometry limits its applicability to two-dimensional channels. To address this, Williams (1963) introduced a theoretical framework for incompressible viscous flow in slender pipes, where the radius varies slowly in the axial direction. This slender approximation, in which radial pressure gradients vanish to leading order, yields a parabolic system closely analogous to boundary-layer theory. Subsequent extensions (Blottner 1977; Daniels & Eagles 1979; Eagles 1982; Kotorynski 1995) clarified the mathematical structure of the model and demonstrated its utility in describing compressible and incompressible flows with mild axial area variation.

Several analytical and numerical investigations have attempted to capture the development of flows in converging and diverging channels. Atabek (1973) provided an approximate analytical solution for converging geometries, while Dennis *et al.* (1997) demonstrated that diverging channels can support multiple steady solutions, with branch selection depending sensitively on the inlet profile. Garg & Maji (1987) and Mutama & Iacovides (1993) employed full numerical simulations to characterize developing flows in converging–diverging geometries, while Gepner & Floryan (2016) investigated periodic converging–diverging channels, showing how repeated contractions and expansions reorganize the developing profile and enhance mixing. Diverging geometries have also been examined in the context of stability: Sahu & Govindarajan (2005) demonstrated that even a small divergence introduces a finite critical Reynolds number, in contrast to the unconditional linear stability of straight-pipe flow; this prediction was later confirmed experimentally by Peixinho & Besnard (2013). More recent computational studies (Sparrow *et al.* 2009) mapped the onset of separation in diffusers, demonstrating that laminar flows at modest Reynolds numbers are far more sensitive to divergence angle than previously assumed.

Despite the extensive body of work on developing flows in straight pipes and quasi-developed flows in slender channels, to the author’s knowledge, a comprehensive theoretical

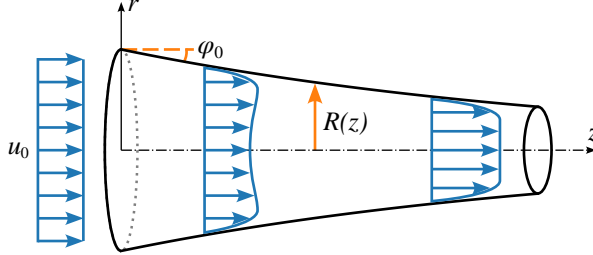


Figure 1: Schematic representation of a converging slender pipe.

description of the hydrodynamic entrance region within slender converging pipes has yet to be developed. Although numerical methods can solve for these flows, a robust analytical model is essential for providing fundamental physical understanding and a rapid predictive tool. Moreover, the model must capture the near-wall velocity overshoot, which is caused by the fluid's near-wall deceleration driving an axial acceleration in an annular region, resulting in the local velocity temporarily exceeding the centerline velocity (Fig. 1).

Building on the two-region model of the entrance in straight pipes presented by Kim (2024) and embedding it within the slender-channel framework of Williams (1963), this work develops a complete analytical description of the developing laminar flow in pipes with mild convergence (Fig. 1). The model divides the cross-section into a wall shear layer, dominated by viscous diffusion and pressure gradient, and an inertia-decaying core, where inertia and viscosity interact. Matching conditions across the interface ensures continuity of velocity and shear. This yields closed-form expressions for the velocity field, pressure gradient, and entrance length as functions of Reynolds number and wall slope. Comparisons with numerical simulations of the laminar Navier–Stokes equations confirm the validity of the theory for converging pipes.

This work thus provides a compact analytical model that bridges classical entrance-region theory with slender-pipe formulations. It clarifies the relationship between boundary-layer growth and axial pressure gradients in axially varying geometries, while offering a predictive tool of immediate relevance to engineering design and fundamental flow studies.

2. Theoretical Model

The developing flow of a viscous, incompressible fluid in an axisymmetric slender pipe is governed by the steady conservation of mass and linear momentum equations. For flows with moderate to high inlet Reynolds numbers, $Re_0 \gg 1$, the conservation equations of mass and linear momentum in the axial and radial direction are given in non-dimensional form, respectively, as

$$\frac{\partial u}{\partial z} + \frac{1}{r} \frac{\partial}{\partial r} (rv) = 0 \quad (2.1a)$$

$$u \frac{\partial u}{\partial z} + v \frac{\partial u}{\partial r} = - \frac{\partial p}{\partial z} + \frac{2}{Re_0} \left[\frac{1}{r} \frac{\partial}{\partial r} \left(r \frac{\partial u}{\partial r} \right) \right] \quad (2.1b)$$

$$\frac{\partial p}{\partial r} = 0 \quad (2.1c)$$

where u and v are the axial and radial velocity components scaled by the inlet average velocity \hat{U}_0 . The hat decorator ($\hat{\cdot}$) represents dimensional quantities. The pressure p is scaled by the dynamic pressure $\hat{\rho} \hat{U}_0^2$, where $\hat{\rho}$ is the fluid density, and r and z are the radial and axial

coordinates scaled by the inlet pipe radius \hat{R}_0 . The flow Reynolds number is defined as $Re_0 = 2\hat{R}_0\hat{U}_0/\hat{\nu}$, where $\hat{\nu}$ is the kinematic viscosity.

To account for the slowly varying pipe radius, the coordinate transformation proposed by Williams (1963) is employed,

$$\xi = z \quad \text{and} \quad \eta = \frac{r}{R(\xi)} \quad (2.2)$$

where $R(\xi)$ is the non-dimensional local pipe radius. Following the approach of Kim (2024), the flow is divided into two radial regions: an inertia-decaying core ($0 \leq \eta \leq \eta_\delta$) and a wall shear layer ($\eta_\delta \leq \eta \leq 1$), where $\eta_\delta(\xi)$ is the interface between the regions.

In the inertia-decaying core, the axial momentum equation, Eq. (2.1b), is approximated as

$$\frac{1}{2} \frac{du_0^2}{d\xi} = -\frac{dp}{d\xi} + \frac{1}{R^2} \frac{2}{Re_0} \left[\frac{1}{\eta} \frac{\partial}{\partial \eta} \left(\eta \frac{\partial u_c}{\partial \eta} \right) \right] \quad (2.3)$$

where u_c is the axial velocity in the inertia-decaying core and $u_0(\xi)$ is the axial velocity at the centerline ($\eta = 0$). In the wall shear layer, advection is neglected, and the momentum balance simplifies to

$$0 = -\frac{dp}{d\xi} + \frac{1}{R^2} \frac{2}{Re_0} \left[\frac{1}{\eta} \frac{\partial}{\partial \eta} \left(\eta \frac{\partial u_w}{\partial \eta} \right) \right] \quad (2.4)$$

where u_w is the axial velocity in the wall region. The velocity field is subject to the no-slip condition at the wall, $u_w(1, \xi) = 0$, and symmetry at the centerline, $\partial u_c / \partial \eta|_{\eta=0} = 0$. At the interface $\eta = \eta_\delta$, the velocity and its radial gradient are continuous:

$$u_c(\eta_\delta, \xi) = u_w(\eta_\delta, \xi) \quad \text{and} \quad \left. \frac{\partial u_c}{\partial \eta} \right|_{\eta_\delta} = \left. \frac{\partial u_w}{\partial \eta} \right|_{\eta_\delta} \quad (2.5)$$

2.1. Analytical Solution

The velocity profiles for the two regions are obtained from Eqs. (2.3) and (2.4). Integrating Eq. (2.4) for the wall shear layer and applying the no-slip condition yields

$$u_w(\eta, \xi) = \frac{Re_0}{8} \frac{dp}{d\xi} R^2 (\eta^2 - 1) + a_1 \ln \eta \quad (2.6)$$

where a_1 is an integration constant. Similarly, integrating Eq. (2.3) for the inertia-decaying core and applying the centerline symmetry condition gives

$$u_c(\eta, \xi) = \frac{Re_0}{8} R^2 \left(\frac{1}{2} \frac{du_0^2}{d\xi} + \frac{dp}{d\xi} \right) \eta^2 + b_2 \quad (2.7)$$

where b_2 is an integration constant. Applying the interface conditions, Eq. (2.5), allows for the determination of a_1 and b_2 .

Denoting

$$D_u = Re_0 \left(\frac{1}{2} \frac{du_0^2}{d\xi} \right) R^4 \quad \text{and} \quad D_p = Re_0 \left(-\frac{dp}{d\xi} \right) R^4 \quad (2.8)$$

which represent dimensionless parameters related to inertial effects and axial pressure drop,

the resulting velocity profiles are obtained as

$$u_c = u_0(1 - \eta^2) + \frac{D_u}{8} \left[(1 - \eta_\delta^2) + \eta_\delta^2 \ln \eta_\delta^2 \right] \left(\frac{\eta}{R} \right)^2 \quad (2.9)$$

$$u_w = u_c + \frac{D_u}{8} \left[1 - \left(\frac{\eta}{\eta_\delta} \right)^2 + \ln \left(\frac{\eta}{\eta_\delta} \right)^2 \right] \left(\frac{\eta_\delta}{R} \right)^2 \quad (2.10)$$

whereas the axial pressure drop is determined as

$$D_p = 8R^2 u_0 + D_u \left(1 - \ln \eta_\delta^2 \right) \eta_\delta^2 \quad (2.11)$$

To solve for the unknowns $u_0(\xi)$ and $\eta(\xi)$, two governing ordinary differential equations (ODEs) are derived. Applying the global mass conservation constraint, $\int_0^1 u \eta d\eta = 1/(2R^2)$, yields an algebraic relation for D_u ,

$$D_u = \frac{8(R^2 u_0 - 2)}{\eta_\delta^2 (1 - \eta_\delta^2 + \ln \eta_\delta^2)} \quad (2.12)$$

The Kármán-Pohlhausen momentum integral technique is applied to the governing equations, resulting in an equation for the axial evolution of the global momentum, $\Theta(\xi) = R^2 \int_0^1 u^2 \eta d\eta$,

$$\frac{d\Theta}{d\xi} = \frac{D_u \eta_\delta^2}{2Re_0 R^2} \quad (2.13)$$

The integral for $\Theta(\xi)$ is evaluated using the velocity profiles from Eqs. (2.9) and (2.10), yielding a complex algebraic expression

$$\Theta(\xi) = R^2 \left\{ \frac{u_0^2}{6} + \frac{1}{12} \left[\frac{5 - \eta_\delta^2(4 + \eta_\delta^2) + (5 + 2 \ln \eta_\delta^2 + \eta_\delta^4) \ln \eta_\delta^2}{(1 + \ln \eta_\delta^2 - \eta_\delta^2)^2} \left(u_0 - \frac{2}{R^2} \right)^2 + \right. \right. \\ \left. \left. - \frac{5 + \eta_\delta^2(\eta_\delta^2 - 6) + 4 \ln \eta_\delta^2}{1 + \ln \eta_\delta^2 - \eta_\delta^2} \left(u_0 - \frac{2}{R^2} \right) u_0 \right] \right\} \quad (2.14)$$

The system is closed by combining Eq. (2.12) with the definition of D_u , Eq. (2.8), which provides an ODE for u_0 . The resulting system of first-order ODEs for u_0 and Θ is solved numerically in Python using the SciPy wrapper to the LSODA Fortran solver from ODEPACK (Hindmarsh 1983), where η_δ is determined iteratively from Eq. (2.14) [using SciPy's implementation of Brent's root finding method (Brent 2013)] at each axial step. The system is integrated starting from $\xi = 0$ with initial conditions corresponding to a uniform inlet profile, namely $u_0(0) = 1$ [since $R(0) = 1$] and $\Theta(0) = 1/2$, which is obtained from the global momentum integral.

3. Results and Discussion

The analytical model is evaluated for Reynolds numbers $Re_0 = 250$ and 500 . This model applies to pipes with a gradual change in radius along the length, but we will concentrate on the results for conditions where the axial velocity becomes self-similar after the flow development region, specifically for determining the entrance length. As a result, the pipe geometry is defined by the tangent of the inlet angle φ_0 (or $dR/d\xi|_0$), with values between -2° (-0.03492) and 0° (straight pipe) being considered.

Results are presented to first establish the theoretical consistency of the model in the

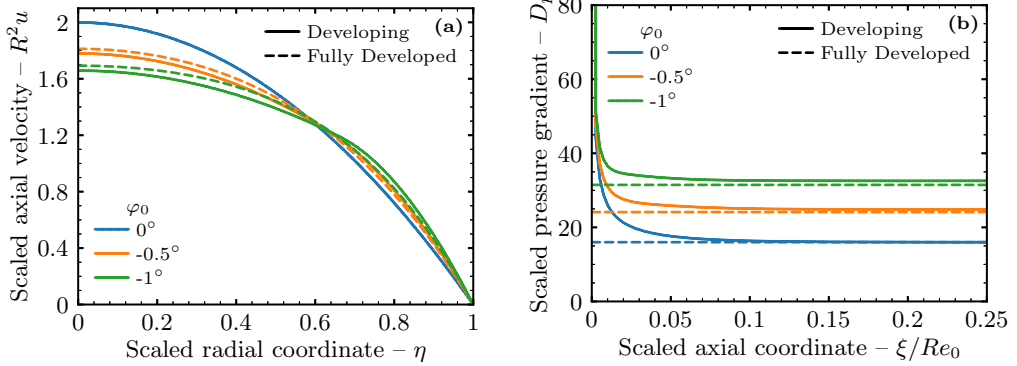


Figure 2: Comparison between developing (solid lines) and fully developed (dashed lines) solutions at selected inlet angles for $Re_0 = 250$. (a) Radial scaled axial velocity profiles, and (b) Axial scaled pressure gradient profiles.

fully developed limit, followed by an analysis of the developing flow characteristics and a validation against numerical simulations.

3.1. Asymptotic Behaviour: Comparison with Fully Developed Flow

To validate the present model, its asymptotic behaviour is investigated by comparing the solution in the far-downstream region with the classical similarity solution for fully developed flow in slender pipes (Williams 1963). For a fully developed flow, the velocity components can be expressed in terms of a similarity function $F(\eta)$ as $u = F/R^2$ and $v = (dR/d\xi)\eta F/R^2$. Substituting these expressions into the momentum equation yields the governing ordinary differential equation (Sauer & Fachini 2024)

$$F'' + \frac{1}{\eta}F' + BF^2 = -\frac{\alpha}{2} \quad (3.1)$$

where $B = Re_0(1/R)(dR/d\xi)$ and $\alpha = Re_0(-dp/d\xi)R^4$ are constants, requiring that

$$R(\xi) = \exp(B\xi/Re_0) \quad (3.2)$$

For a given B , the pressure gradient parameter α is an eigenvalue of the problem. The solution of Eq. (3.1) is determined considering the boundary conditions $F(1) = 0$, $F'(0) = 0$ and $F(0) = F_0$. The similarity function $F(\eta)$ is obtained iteratively by adjusting the parameter F_0 to satisfy the condition $\int_0^1 F\eta d\eta = 1/2$.

As $\xi \rightarrow \infty$, the developing flow must converge to a self-similar state. This implies that the scaled axial velocity profile from the present model, $R(\xi)^2 u(\eta, \xi)$, should approach the similarity function $F(\eta)$. Concurrently, the dimensionless pressure gradient parameter from the developing model, $D_p(\xi)$, should converge to the constant eigenvalue α of the fully developed problem.

Figure 2a compares the asymptotic velocity profile from the developing flow model with the fully developed similarity solution for a converging pipe at $Re_0 = 250$ for $\varphi_0 = 0^\circ$, -0.5° , and -1° . The dashed lines represent the fully developed solution $F(\eta)$, whereas the solid lines show the developing flow solution $R^2 u$ evaluated at a large axial distance ($\xi/Re_0 = 0.25$). A small deviation between the profiles is observed near $\eta = 0.5$. This is inherent to the two-region approximation, which imposes continuity of the function and its first derivative but does not guarantee continuity of higher-order derivatives at the interface η_δ . However,

Re_0	φ_0	B	ℓ_e/Re_0	Pressure Gradient			Centerline Velocity		
				α	D_p	% Diff.	F_0	R^2u_0	% Diff.
Laminar	0.0	0.00	0.1174	16.00	16.00	0.03	2.00	2.00	0.02
250	-0.5	-2.18	0.1027	24.13	24.80	2.81	1.81	1.78	1.81
	-1.0	-4.36	0.0764	31.47	32.55	3.43	1.69	1.66	2.07
	-1.5	-6.55	0.0610	38.36	39.74	3.59	1.61	1.58	1.91
	-2.0	-8.73	0.0502	44.96	46.58	3.60	1.55	1.52	1.63
500	-0.5	-4.36	0.0764	31.47	32.55	3.43	1.69	1.66	2.07
	-1.0	-8.73	0.0502	44.95	46.57	3.60	1.55	1.52	1.63
	-1.5	-13.09	0.0364	57.53	59.55	3.51	1.46	1.44	1.06
	-2.0	-17.46	0.0289	69.59	71.94	3.37	1.40	1.39	0.60

Table 1: Comparison of developing flow model parameters with the fully developed similarity solution. Functions D_p and R^2u_0 evaluated at $\xi/Re_0 = 0.25$.

the general agreement confirms that the developing flow solution converges to the fully developed profile.

The convergence of the pressure gradient parameter is shown in Fig. 2b for $Re_0 = 250$. The value of D_p from the developing model is plotted against the axial coordinate ξ/Re_0 . Horizontal (asymptotic) dashed lines representative of the pressure drop α for fully developed flow are also included. It is observed that D_p rapidly approaches the fully developed solution for $\varphi_0 = 0^\circ, -0.5^\circ$, and -1° .

A quantitative comparison of the asymptotic pressure gradient parameter is presented in Table 1 for Re_0 of 250 and 500 at several inlet angles φ_0 . The table lists the eigenvalue α obtained from the fully developed model and the asymptotic value of D_p (at $\xi/Re_0 = 0.25$) from the present developing flow model. The relative difference is less than 4 % for all cases. The scaled centerline velocity values for the fully developed (F_0) and developing (R^2u_0) solutions are also shown. The relative difference of 2 % or less demonstrates good agreement between solutions, confirming the consistency of the present model with the established theory for fully developed slender pipe flows.

3.2. Developing Flow Characteristics

Upon confirmation that the solution derived from the analytical model accurately represents the results for the fully developed region, the subsequent focus shifts to analyzing the developing flow.

Figure 3a shows the evolution of the centerline velocity, u_0 , along the non-dimensional axial coordinate, ξ/Re_0 , for selected geometries at $Re_0 = 250$. In all cases, the centerline velocity accelerates from its initial value and approaches an asymptotic, fully developed value. For the straight pipe, u_0 approaches the classical value of 2.0. The converging geometries, with their favourable pressure gradient, cause a more rapid acceleration and a shorter hydrodynamic entrance length, ℓ_e , which is assumed as the axial location where $R^2u_0(\ell_e) = 0.99F_0$ (Kim 2024). As the convergence angle increases ($B \ll -1$), the effect of the strong favourable pressure gradient becomes dominant, leading to the expected rapid decrease in entrance length. The following polynomial fitting of degree two is obtained for the interval $-17.5 \leq B \leq 0$, considering the values from Table 1,

$$\frac{\ell_e}{Re_0} = 3.045 \times 10^{-4} B^2 + 1.033 \times 10^{-2} B + 0.1174, \quad -17.5 \leq B \leq 0 \quad (3.3)$$

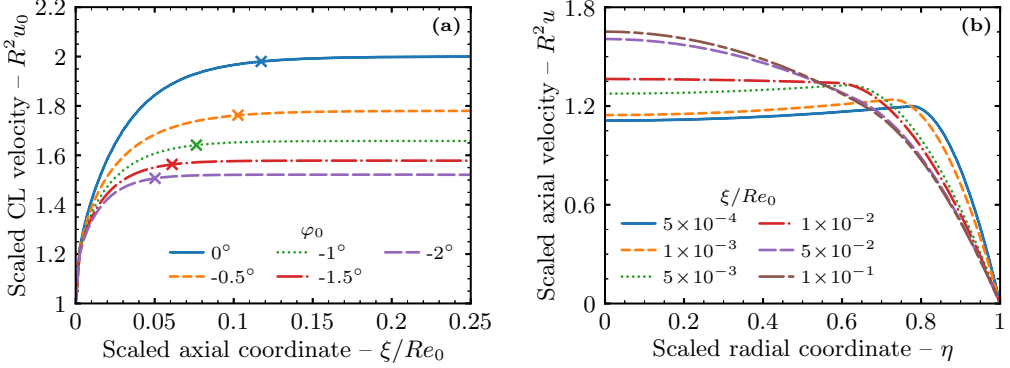


Figure 3: Axial velocity profiles for $Re_0 = 250$. (a) Centerline profiles at selected inlet angles, and (b) Profiles at selected axial positions for $\varphi_0 = -1^\circ$. Markers \times denote the inlet length ℓ_e/Re_0 for each case.

which can be used to predict ℓ_e . The root mean square error fitting is about 0.1 %.

The development of the axial velocity profile, u , is shown in Fig. 3b for the converging case with $Re_0 = 250$ and an inlet angle of -1° at selected axial locations. Near the inlet ($\xi/Re_0 \ll 1$), the velocity profile is relatively flat in the core. An overshoot in velocity is observed, similar to what is seen in straight pipes. As the flow moves downstream, the boundary layer grows, and the profile gradually evolves toward its fully developed shape. The resulting profile is less parabolic (more plug-like) than the Poiseuille profile. This is a direct consequence of the favourable pressure gradient, which accelerates the core flow relative to the fluid near the wall, creating a more uniform velocity distribution across the central region (cf. Table 1).

3.3. Numerical Validation

To validate the analytical model, solutions for selected cases are compared against numerical simulations obtained using the commercial software ANSYS® Fluent 2024 R1. The numerical analysis solves the full laminar Navier-Stokes equations, including axial diffusion and radial pressure gradients, in a three-dimensional domain. The mesh is generated in ANSYS® SpaceClaim using an O-type structured grid in the cross-section with refinement at the pipe inlet and walls to account for flow development and boundary-layer effects, resulting in an average of 10×10^6 hexahedral cells. The Coupled algorithm is used for pressure-velocity coupling, whereas a second-order upwind method is selected for the momentum fluxes. A uniform axial velocity profile is specified at the inlet ($z = 0$) to simulate the developing flow condition, with no-slip stationary wall and pressure-outlet boundary conditions applied to their respective surfaces. A grid independence study was performed, confirming that the mesh resolution is sufficient to ensure results free from significant discretization error.

Figure 4 compares the pressure drop predicted by the analytical model with numerical results for converging geometries at $Re_0 = 500$ and $\varphi_0 = 0^\circ$, -0.5° , and -1° . Figure 4a shows that the centerline velocity u_0 reaches a value of 2.0 in the fully developed region in straight pipes, consistent with classical theory. The converging pipe exhibits a much steeper acceleration, consistent with the analytical results from Section 3.2. The numerical solution at $\xi/Re_0 = 0.25$ matches almost exactly the fully developed solution from Table 1. Furthermore, a slight deviation is observed between the numerical and analytical entrance lengths. Figure 4b displays the numerical and analytical solutions of the scaled axial velocity profile at selected axial locations for $Re = 500$ and $\varphi_0 = -1^\circ$. A larger deviation between

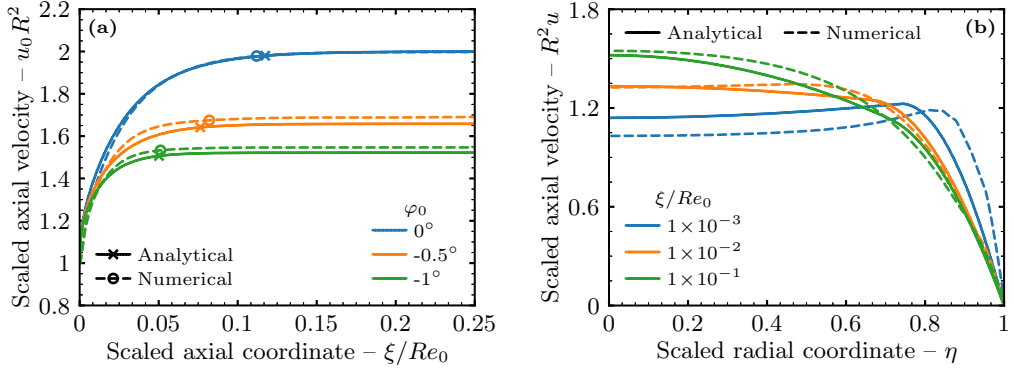


Figure 4: Analytical (solid lines) and numerical (dashed lines) axial velocity solutions for $Re_0 = 500$. (a) Variation in the axial direction for selected φ_0 (markers represent entrance lengths), and (b) Profiles at selected axial positions for $\varphi_0 = -1^\circ$.

numerical and analytical profiles near the entrance ($\xi/Re_0 \ll 1$), which is also observed in straight pipe solutions (Kim 2024). Altogether, the model accurately captures distinct behaviours, further validating its formulation.

4. Conclusion

An analytical model for developing laminar flow in slender converging pipes has been developed. The model extends the classical two-region analysis of Kim (2024) to pipes with slowly varying cross-sections by incorporating the slender-pipe approximation of Williams (1963). The solution provides a complete description of the velocity field and pressure distribution throughout the hydrodynamic entrance region.

The model accurately predicts the evolution of the velocity profile from a uniform inlet condition to a fully developed state. The analytical solutions for centerline velocity, velocity profiles, and pressure drop exhibit good agreement with numerical simulations of the full Navier-Stokes equations for inlet Reynolds numbers of 250 and 500, and inlet angles ranging from -2° to 0° . The pipe geometry has a profound effect on the hydrodynamic entrance length. A converging geometry imposes a favourable pressure gradient that accelerates the flow development, resulting in a shorter entrance length compared to a straight pipe. The solution for the developing flow is shown to asymptotically converge to the classical similarity solution for fully developed slender pipe flow in the far-downstream limit, confirming the theoretical consistency of the model.

The theoretical framework presented herein provides fundamental physical insight into the interplay between viscous boundary layer growth and pressure gradients imposed by varying geometries. Furthermore, it serves as a robust and computationally efficient predictive tool for the design and analysis of systems involving flows in slender non-uniform conduits.

Declaration of interests. The authors report no conflict of interest.

Data availability statement. Data sets generated during the current study are available from the corresponding author on reasonable request.

REFERENCES

ATABEK, H. B. 1973 Development of flow in the entrance region of a converging channel. *Applied Scientific Research* **27** (1), 103–117.

BLOTTNER, F. G. 1977 Numerical solution of slender channel laminar flows. *Computer Methods in Applied Mechanics and Engineering* **11** (3), 319–339.

BRENT, RICHARD P. 2013 *Algorithms for Minimization without Derivatives*. United States: Courier Corporation.

CAMPBELL, WILLIAM D. & SLATTERY, JOHN C. 1963 Flow in the entrance of a tube. *Journal of Basic Engineering* **85** (1), 41–45.

DANIELS, P. G. & EAGLES, P. M. 1979 High Reynolds number flows in exponential tubes of slow variation. *Journal of Fluid Mechanics* **90** (2), 305–314.

DENNIS, S. C. R., BANKS, W. H. H., DRAZIN, P. G. & ZATURSKA, M. B. 1997 Flow along a diverging channel. *Journal of Fluid Mechanics* **336**, 183–202.

DURST, F., RAY, S., ÜNSAL, B. & BAYOUMI, O. A. 2005 The development lengths of laminar pipe and channel flows. *Journal of Fluids Engineering* **127** (6), 1154–1160.

EAGLES, P. M. 1982 Steady flow in locally exponential tubes. *Proceedings of the Royal Society of London. Series A, Mathematical and Physical Sciences* **383** (1784), 231–245, arXiv: 2397359.

FARGIE, D. & MARTIN, B. W. 1971 Developing laminar flow in a pipe of circular cross-section. *Proceedings of the Royal Society of London. A. Mathematical and Physical Sciences* .

GARG, VIJAY K. & MAJI, P. K. 1987 Flow through a converging-diverging tube with constant wall enthalpy. *Numerical Heat Transfer* **12** (3), 285–305.

GEPRNER, STANIS LAW & FLORYAN, J. M. 2016 Flow dynamics and enhanced mixing in a converging–diverging channel. *Journal of Fluid Mechanics* **807**, 167–204.

HAMEL, GEORG 1917 Spiralförmige Bewegungen zäher Flüssigkeiten. *Jahresbericht der Deutschen Mathematiker-Vereinigung* **25**, 34–60.

HINDMARSH, ALAN C. 1983 ODEPACK, a systemized collection of ode solvers. *Scientific Computing* **1**.

JEFFERY, G. B. 1915 L. The two-dimensional steady motion of a viscous fluid. *The London, Edinburgh, and Dublin Philosophical Magazine and Journal of Science* **29** (172), 455–465.

KAKAÇ, S. & ÖZGÜ, M. R. 1969 Analysis of laminar flow forced convection heat transfer in the entrance region of a circular pipe. *Wärme- und Stoffübertragung* **2** (4), 240–245.

KIM, TAIG YOUNG 2024 Analytical solution for laminar entrance flow in circular pipes. *Journal of Fluid Mechanics* **979**, A51.

KOTORYNSKI, W. P. 1995 Viscous flow in axisymmetric pipes with slow variations. *Computers & Fluids* **24** (6), 685–717.

LANGHAAR, HENRY L. 1942 Steady flow in the transition length of a straight tube. *Journal of Applied Mechanics* **9** (2), A55–A58.

LUNDGREN, T. S., SPARROW, E. M. & STARR, J. B. 1964 Pressure drop due to the entrance region in ducts of arbitrary cross section. *Journal of Basic Engineering* **86** (3), 620–626.

McCOMAS, S. T. 1967 Hydrodynamic entrance lengths for ducts of arbitrary cross section. *Journal of Basic Engineering* **89** (4), 847–850.

MOHANTY, A. K. & ASTHANA, S. B. L. 1979 Laminar flow in the entrance region of a smooth pipe. *Journal of Fluid Mechanics* **90** (3), 433–447.

MUTAMA, K. R. & IACOVIDES, H. 1993 The investigation of developing flow and heat transfer in a long converging duct. *Journal of Heat Transfer* **115** (4), 897–903.

PEIXINHO, JORGE & BESNARD, HUGUES 2013 Transition to turbulence in slowly divergent pipe flow. *Physics of Fluids* **25** (11), 111702.

SAHU, KIRTI CHANDRA & GOVINDARAJAN, RAMA 2005 Stability of flow through a slowly diverging pipe. *Journal of Fluid Mechanics* **531**, 325–334.

SAUER, VINICIUS M. & FACHINI, FERNANDO F. 2024 Laminar swirling slender pipe flows. *Physics of Fluids* **36** (10), 103623.

SPARROW, E. M., ABRAHAM, J. P. & MINKOWYCZ, W. J. 2009 Flow separation in a diverging conical duct: Effect of Reynolds number and divergence angle. *International Journal of Heat and Mass Transfer* **52** (13), 3079–3083.

SPARROW, E. M. & LIN, S. H. 1964 The developing laminar flow and pressure drop in the entrance region of annular ducts. *Journal of Basic Engineering* **86** (4), 827–833.

SPARROW, E. M., LIN, S. H. & LUNDGREN, T. S. 1964 Flow development in the hydrodynamic entrance region of tubes and ducts. *Physics of Fluids* **7** (3), 338–347.

VAN DYKE, MILTON 1970 Entry flow in a channel. *Journal of Fluid Mechanics* **44** (4), 813–823.

WILLIAMS, JAMES C. 1963 Viscous compressible and incompressible flow in slender channels. *AIAA Journal* **1** (1), 186–195.